BULLETIN OF THE EARTHQUAKE
RESEARCH INSTITUTE
Vol. 48 (1970), pp. 351-362

21. *Theoretical Seismograms of Spheroidal Type on the Surface of a Gravitating Elastic Sphere. IV. Homogeneous Mantle with a Liquid Core Excited by Colatitudinal Force.*

By Tatsuo USAMI and Yasuo SATÔ,
Earthquake Research Institute.
(Read Dec. 24, 1968.—Received March 31, 1970.)

1. Introduction

Various properties of the waves propagated on the surface of an elastic sphere have been studied to elucidate the nature of both surface and body waves by means of theoretical seismograms. For this purpose the synthetic seismograms based on the normal mode theory were prepared for a number of earth models for the following cases assuming a force on a localized area of the surface:

(1) Torsional disturbance due to a tangential force in the azimuthal direction[1].
(2) Spheroidal mode of disturbance due to a radial force applied on the surface[2].

However, in order to make our study complete on the propagation of seismic waves excited by a force system acting at the source of an earthquake, we are to calculate

(3) The spheroidal oscillation when a colatitudinal stress is applied on the surface.

Here a homogeneous mantle and a liquid core is assumed and the gravity effect is considered as before. The theoretical seismograms representing the disturbances on the surface were calculated by summing up contributions of the free spheroidal oscillations from the fundamental through the tenth radial higher modes with periods larger than 12 seconds. Special attention was paid to the comparative magnitude of excited amplitude between the present problem and the problem of the radial stress studied before. Characteristic features of wave propagation similar to the previous study were also given.

2. Earth Model and the Applied Force

The earth model employed in the present study is common to our previous work[3], in which a radial force is applied on the surface of a circular area around the pole. This work is cited as the case [III] for

simplicity, and the fundamental expressions giving the disturbance are the same, although a different kind of excitation force is assumed. The axial symmetry ($m=0$) is assumed in the numerical calculations. The earth model and the force working at the source are summarized in the Table 1 together with those for the case [III]. Figure 1 also illustrates schematically.

Table 1.

	Present problem	Previous problem (Case [III])
Earth model	Homogeneous mantle and homogeneous liquid core	
Earth's radius	$a=6370$ km	
Core radius	$b=6370-2900=3470$ km	
Density (mantle)	ρ(mantle)$=4.6232$ gr/cm^3	
Density (core)	ρ(core)$=10.171=2.2\times\rho$(mantle)	
Velocity (mantle)	$V(S\text{ wave})=V(P\text{ wave})/\sqrt{3}=6.667$ km/sec	
Velocity (core)	$V(P\text{ wave})=10.00$ km/sec	
Time unit	$2\pi a/V(S\text{ wave})=6000$ sec	
External force	Colatitudinal force $F\widehat{_{r\theta}}=\Theta(\theta,\varphi)\cdot f(t)$ $F\widehat{_{rr}}=0$	Radial force $F\widehat{_{r\upsilon}}=0$ $F\widehat{_{rr}}=\Theta(\theta,\varphi)\cdot f(t)$
$\Theta(\theta,\varphi)=\Theta^0(\cos\theta)$	$\sum T_{mn}\dfrac{d}{d\theta}P_n^m(\cos\theta)\cos m\varphi$ $=\begin{cases}0 & \theta<\theta_1,\ \theta>\theta_2\\ 1 & \theta_1<\theta<\theta_2\end{cases}$	$\sum S_{mn}P_n^m(\cos\theta)\cos m\varphi$ $=\begin{cases}0 & \theta>\theta_1\\ 1 & \theta<\theta_1\end{cases}$
θ_1, θ_2 (radian)	$\theta_1=0.006$, $\theta_2=0.012$	$\theta_1=0.012$ (=86.4 km)
$f(t)$	$\begin{cases}0 & \lvert t\rvert>t_1\\ 1/t_1 & \lvert t\rvert<t_1\end{cases}$	$\begin{cases}0 & \lvert t\rvert>t_1\\ -1/2t_1 & -t_1<t<0\\ 1/2t_1 & 0<t<t_1\end{cases}$
t_1	0.004 (=24 sec)	0.004 (=24 sec)
$f^*(p)$	$2\dfrac{\sin(pt_1)}{pt_1}$	$-i\cdot 4\dfrac{\sin^2(pt_1/2)}{pt_1}$

3. Non-dimensional Frequency, Phase and Group Velocities

In spite of the difference of external force the mode of oscillation in the previous and the present problems are the same. Consequently the non-dimensional frequency, and the phase and group velocities calculated from it by simple formulas are commonly used in two problems.

4. Common Spectrum

The Common Spectrum for the radial and colatitudinal displacements are given by the following formulas as before

$$
{}_iS_n^{\,u} = \left(\frac{S_{mn}}{dE_S/dp} + \frac{T_{mn}}{dE_T/dp}\right) U_n(a)\cdot f^*(p)\ ,
$$

$$
{}_iS_n^{\,v} = \left(\frac{S_{mn}}{dE_S/dp} + \frac{T_{mn}}{dE_T/dp}\right) V_n(a)\cdot f^*(p)\ . \tag{4.1}
$$

In the expression (4.1), $f^*(p)$ the Fourier transform of the function $f(t)$, has the form

$$
f^*(p) = 2\frac{\sin(pt_1)}{pt_1}\ . \tag{4.2}
$$

S_{mn} is zero in the present case, while T_{mn}, the coefficient of $dP_n^{\,m}(\cos\theta)/d\theta$ in the expansion of the function $\Theta^0(\cos\theta)$, can be calculated from the equation given in the tenth row of Table 1. The formulas giving radial distribution of U_n and V_n, used for the case [III] are also applicable here. The radial and colatitudinal components of the Common Spectrum are shown in Figures 2-a and 2-b. If we compare these Common Spectra in two cases remembering that the ordinate scale is not different, it is remarkable that the amplitude for the present case is much smaller (order of 1/10 in average) than that for the case [III]. The difference of the area and the magnitude of the applied force, which is found in Figure 1, cannot explain the difference mentioned above, and it will be due to the following reason. For the present case T_{mn} is given by

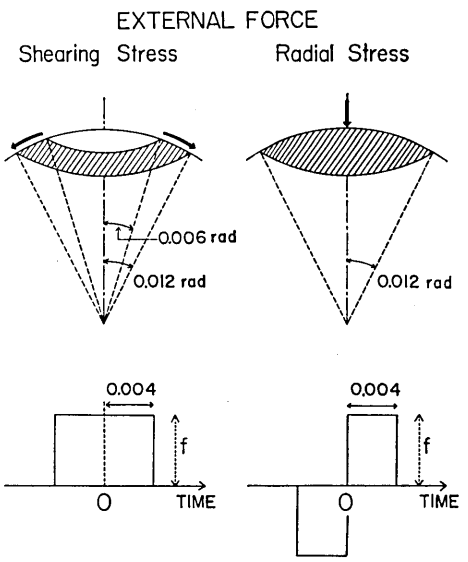

Fig. 1. Schematic figure showing the time and space function of applied force for the present case (left) and the case [III] (right).

$$
T_{mn} = -\frac{2n+1}{2n(n+1)}\int_{-1}^{1}\Theta^0(\cos\theta)P_n^{\,1}(\cos\theta)\,d(\cos\theta)\ , \tag{4.3}
$$

while for the case [III]

$$
S_{mn} = \frac{2n+1}{2}\int_{-1}^{1}\Theta^0(\cos\theta)\,P_n(\cos\theta)\,d(\cos\theta)\ . \tag{4.4}
$$

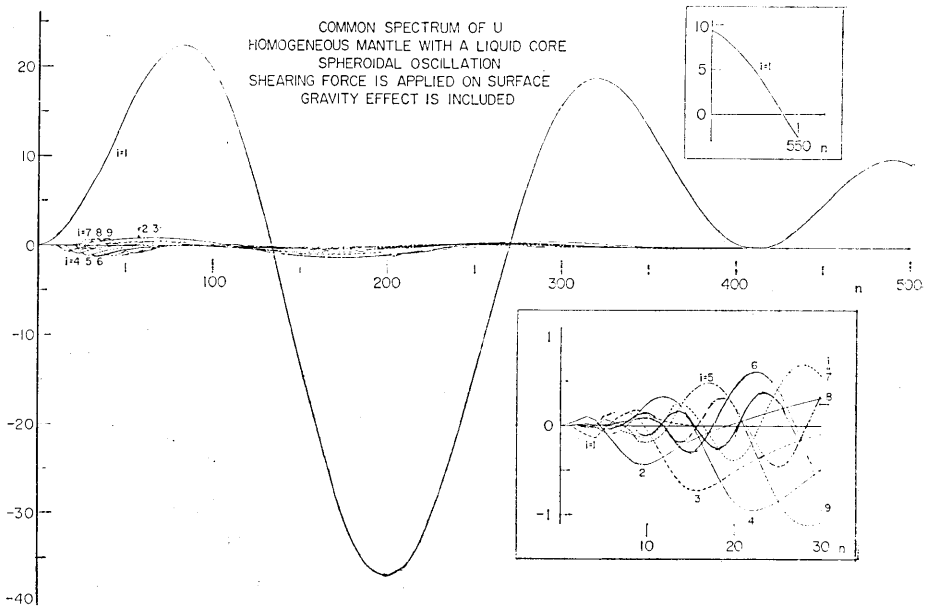

(a)

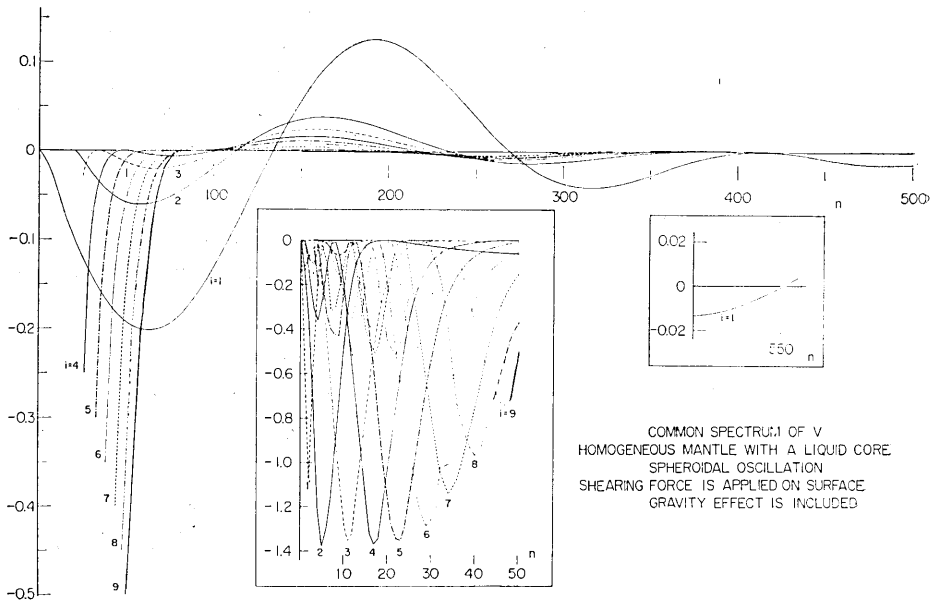

(b)

Fig. 2. Radial and colatitudinal components of the Common Spectrum. Unit of ordinate scale is same with the case [III]. It is remarkable that the colatitudinal spectra for radial higher modes exceed the amplitude of spectrum for the fundamental mode at the period larger than 120 sec.

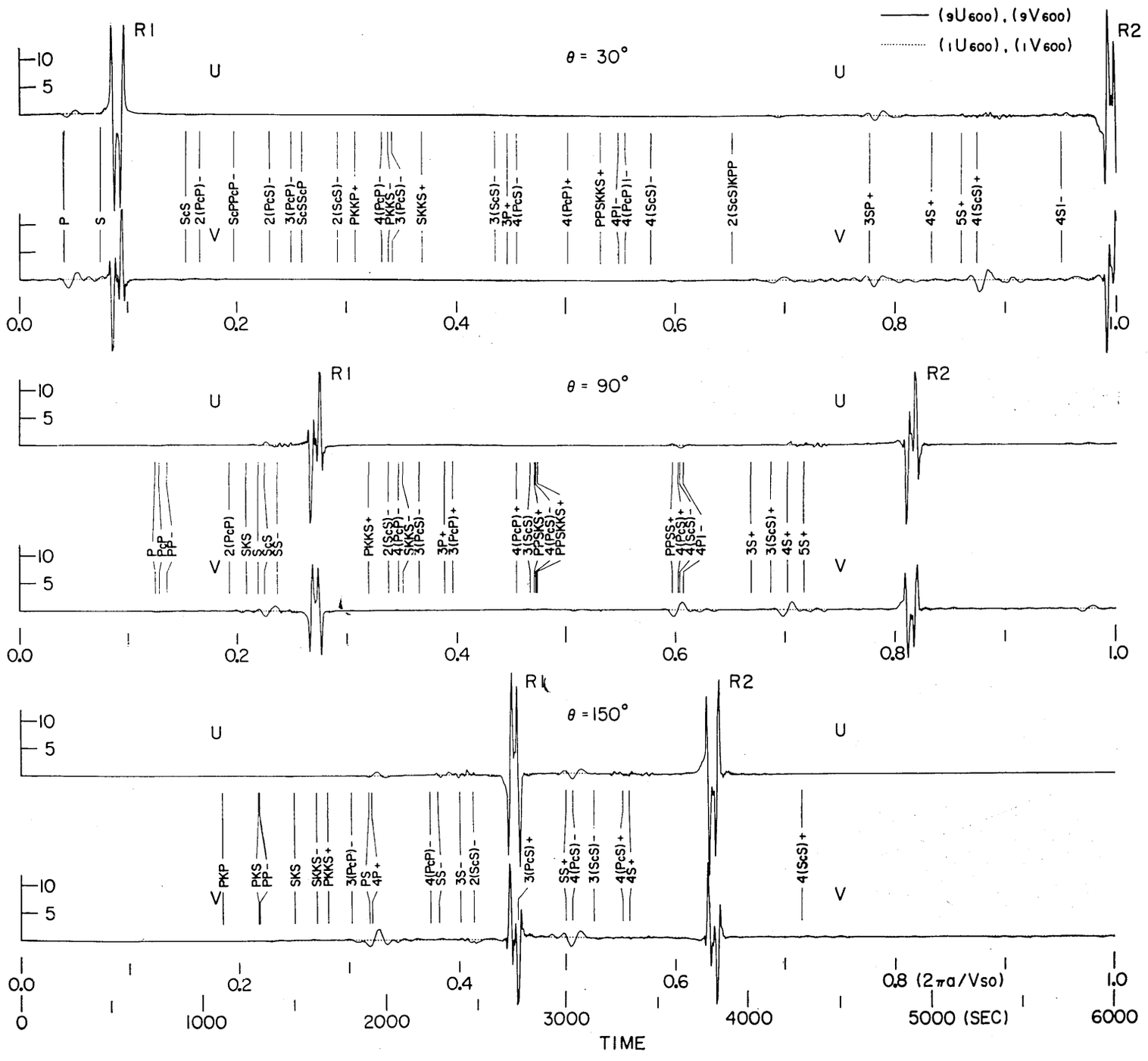

Fig. 3. Theoretical seismograms of spheroidal disturbances on the surface of an elastic mantle with a liquid core. *R1*, *R2* mean Rayleigh waves. The expected arrivals of various body phases calculated from a simple theory of geometrical optics are shown by arrows. The unit of time is that for *S* wave to circle the globe, namely, $2\pi a/Vso=6000$ sec. The unit of ordinate scale is same as the case [III].

When n is large $P_n^1(\cos\theta)$ is the order of $n \cdot P_n(\cos\theta)$, hence T_{mn} is a quantity of the order of S_{mn}/n. Since

$$\frac{\partial E_S}{\partial p} = n(n+1)\frac{V_n(a)}{U_n(a)}\frac{\partial E_T}{\partial p}^{4)} ,$$

the ratio of common spectra of the present case and the case [III] is given as

$$(n+1)\,V_n(a)\cdot f^*(p)/U_n(a)\cdot f^*_{\mathrm{III}}(p) .$$

Figure 2 show that for the radial component, the Common Spectrum of the fundamental mode has a maximum far larger than those of the higher radial modes, while for the colatitudinal component the relation is reversed. The maximum values of the radial higher modes decrease rather gradually with the mode number i, implying that the accuracy of the theoretical seismogram expressing body waves will be improved by adding extra radial higher modes with $i>10$. The Common Spectrum decreases with the increase of colatitudinal order number n and becomes negligibly small when $n>500$ for the fundamental mode, and $n>300$ for the higher modes.

5. Theoretical Seismogram

Theoretical seismograms are calculated by summing up contributions from various modes. The largest value of the colatitudinal order number n employed in the synthesis are same as that for the case [III]. The seismograms at 13 points on the surface for the time interval $t=0.001$ (0.001) 1.000 are shown in Figures 3, 4 and 5.

Figure 3 shows that the body wave amplitude relative to that of surface wave is much larger in this case than in the case [III]. In Figure 4, in which the seismograms for the case [III] are also shown for comparison, the expected arrival times based on the simple theory of geometrical oplics are shown by arrows, which agree satisfactorily with the apparent arrival of body waves. The amplitude of body waves is 1/5~1/10 of the corresponding waves of the case [III], reflecting the smallness of spectral amplitudes in the present problem. This fact suggests that the spheroidal disturbance, especially short period modes, are hard to be excited by the application of colatitudinal force. The radial component of body waves is larger than that of the colatitudinal one for the case [III], while in the present case the relation is reversed. In Figure 5, which consists of only radial higher modes, *ScS* wave can be traced with slight change of the wave forms.

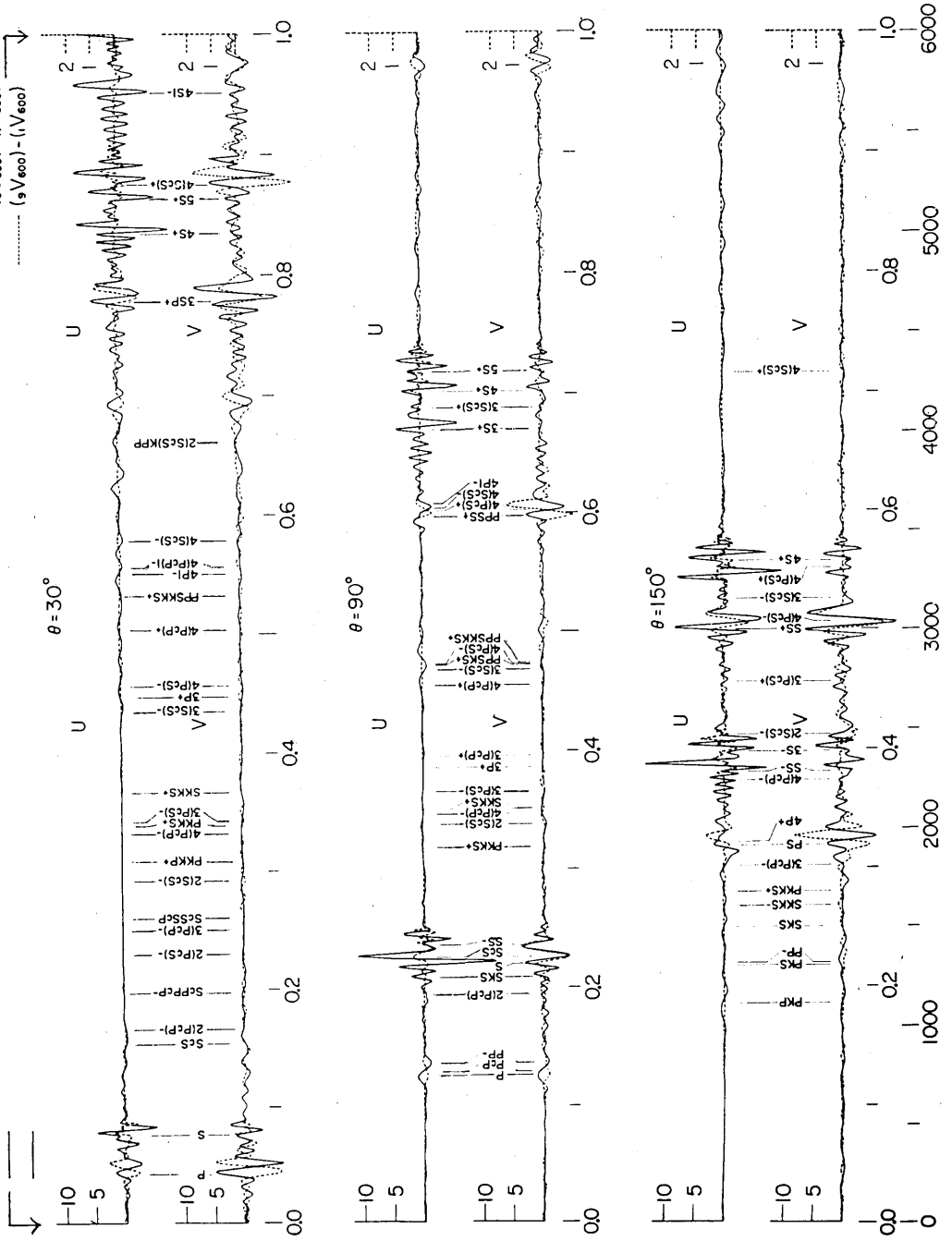

Fig. 4. Theoretical seismogram of spheroidal disturbance consisting of only radial higher modes. Solid line refers to the case [III] and the broken line is the present case. Ordinate scale: left side—case [III], right side—present case. Note the amplitude ratio between two cases.

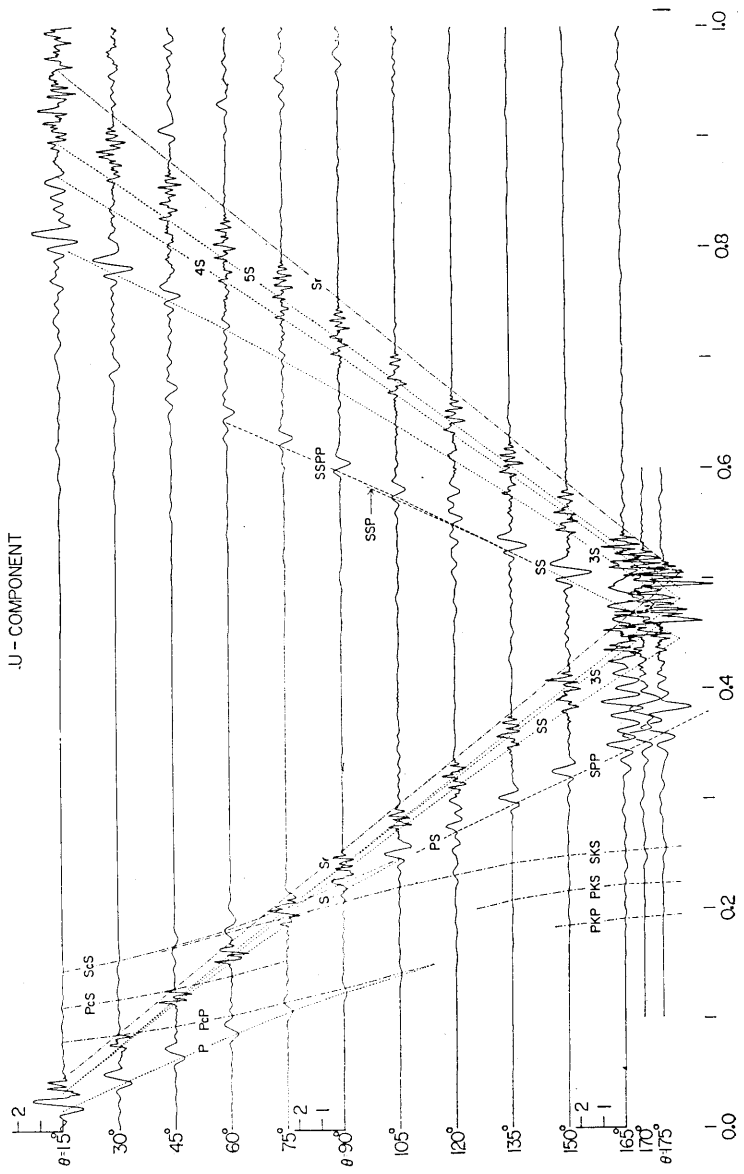
U - COMPONENT
θ=15°
30°
45°
60°
75°
θ 90°
105°
120°
135°
150°
165°
170°
θ=175°
P
PcP
Pc-S
ScS
S
Sr
4S
5S
Sr
SSPP
SSP
PS
SS
3S
SS
3S
SPP
PKP PKS SKS
0.0
0.2
0.4
0.6
0.8
1.0

Fig. 5 (a)

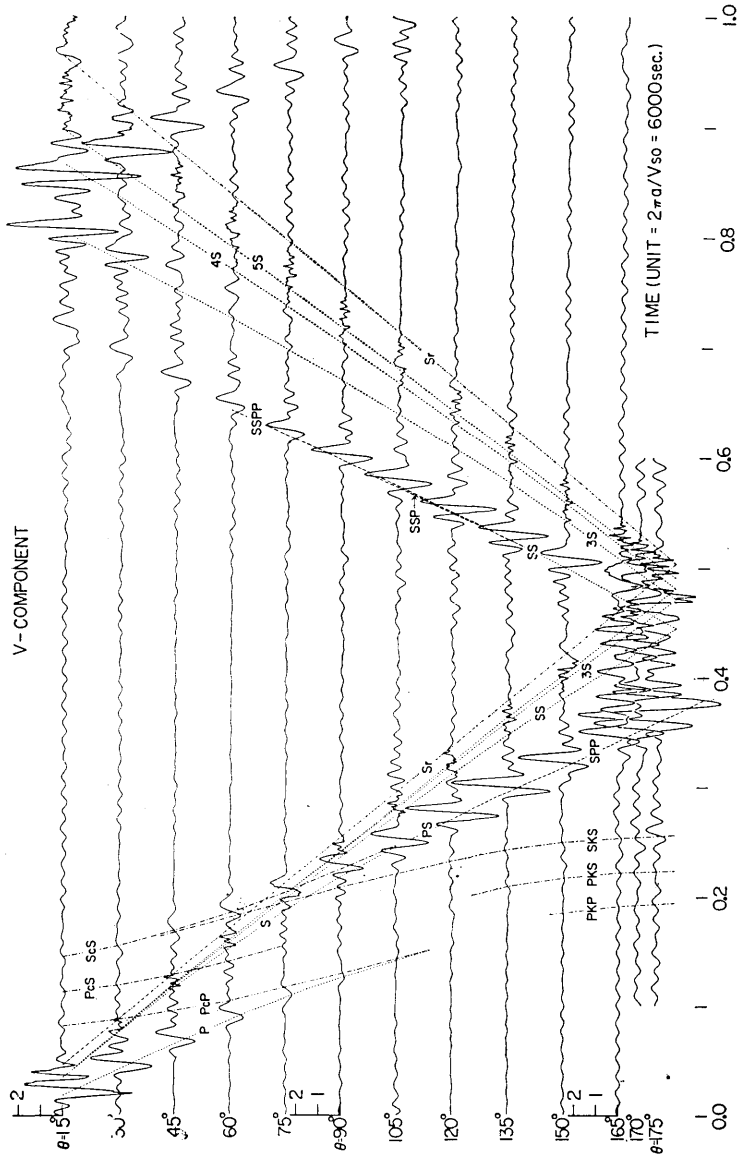

Fig. 5 (b)

Fig. 5. Theoretical seismogram consisting of the radial higher modes only. Theoretical travel time curve of various body phases are given in the figure. S_r is the travel time curve of S wave propagated along the surface of the sphere.

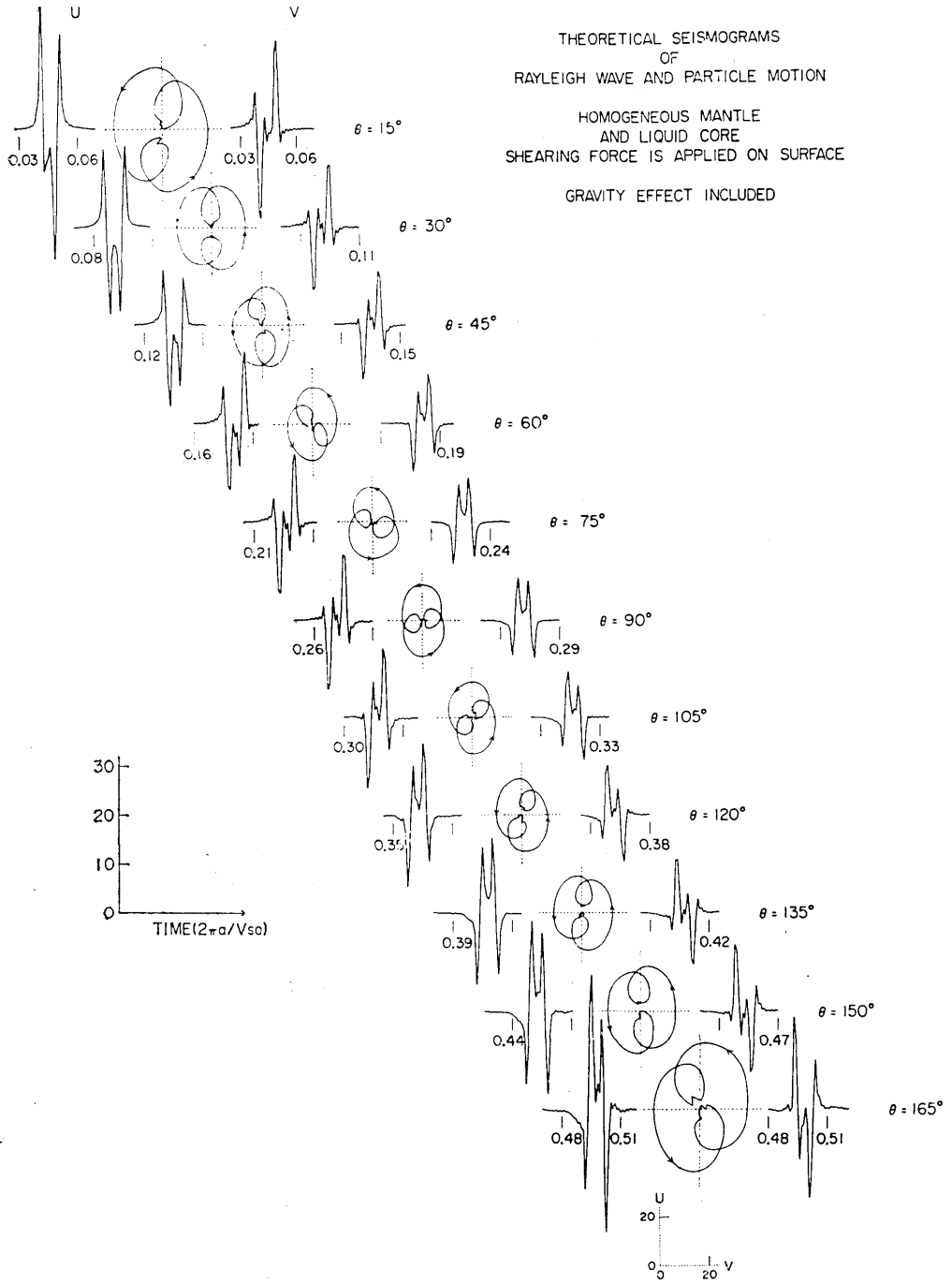
U
V
THEORETICAL SEISMOGRAMS
OF
RAYLEIGH WAVE AND PARTICLE MOTION
HOMOGENEOUS MANTLE
AND LIQUID CORE
SHEARING FORCE IS APPLIED ON SURFACE
GRAVITY EFFECT INCLUDED
θ = 15°
θ = 30°
θ = 45°
θ = 60°
θ = 75°
θ = 90°
θ = 105°
θ = 120°
θ = 135°
θ = 150°
θ = 165°
0.03
0.06
0.03
0.06
0.08
0.11
0.12
0.15
0.16
0.19
0.21
0.24
0.26
0.29
0.30
0.33
0.35
0.38
0.39
0.42
0.44
0.47
0.48
0.51
0.48
0.51
30
20
10
0
TIME(2πa/Vs0)
U
20
0
0
20
V

Fig. 6 (a)

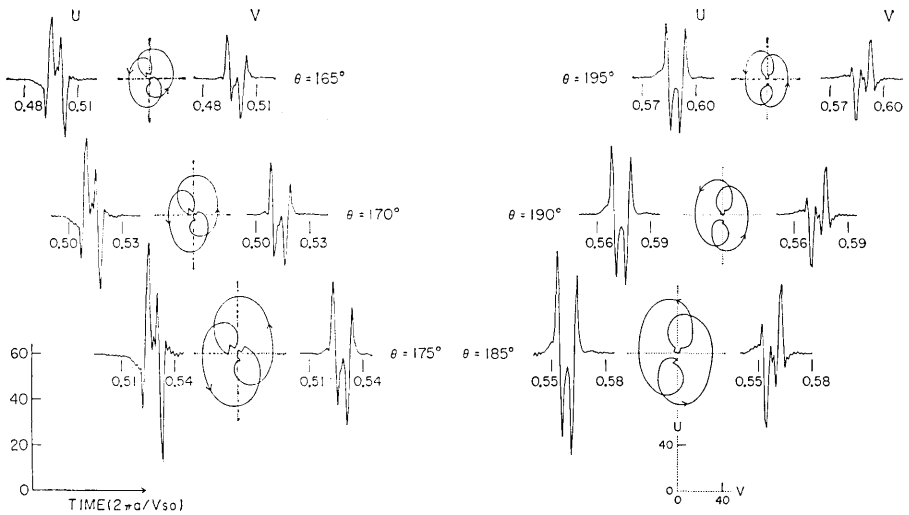

Fig. 6 (b)

Fig. 6. Theoretical seismogram of Rayleigh wave and its orbital motion computed from the fundamental mode. (The scale of the orbital motion is half of that for disturbance.) The peculiar feature of particle motion like a combination of two ellipses is due to the space and time function of external force. The direction of line connecting the loop of the loci changes gradually as the epicentral distance increases and is subjected to a sudden change of $\pi/2$ at the passage of antipode. This can be understood as the polar phase shift phenomenon on a spherical surface.

6. Analysis of Rayleigh Waves

Analysis of Rayleigh wave similar to that in the case [III] is carried out in this study, too. Figures 6-a and 6-b, which are the results of the superposition of fundamental mode, show the disturbance near the passage of Rayleigh wave and its loci of particle motion. The peculiar form of particle orbit indicating a combination of two ellipses is due to the temporal and spatial distribution of the applied force. Each ellipse exhibits typical characteristics of Rayleigh waves along the plane surface of a homogeneous half space: namely (1) elliptic orbit, (2) retrograde particle motion and (3) amplitude ratio of the vertical and horizontal displacements, which is nearly equal to the theoretical value of 1.46. The amplitude becomes larger as the station approaches the pole and antipode, which fact is a characteristic feature of surface waves on a sphere. The line representing the direction of the loop of loci rotates gradually as the epicentral distance increases and jumps abruptly at the antipode by the angle $\pi/2$. This fact can be interpreted as the polar phase shift phenomenon on a spherical surface.

Acknowledgements

The numerical calculation was carried out by HITAC 5020E at the Computer Centre of the University of Tokyo and IBM 7090 through the project UNICON.

References

1) Y. SATÔ, T. USAMI, M. LANDISMAN and M. EWING, "Basic Study on the Oscillation of a Sphere Part V: Propagation of Torsional Disturbances on a Radially Heterogeneous Sphere. Case of a Homogeneous Mantle with a Liquid Core," *Geophys. J.*, **8** (1963), 44-63.
Y. SATÔ, T. USAMI and M. LANDISMAN, "Theoretical Seismograms of Torsional Disturbances Excited at a Focus within a Heterogeneous Spherical Earth—Case of a Gutenberg-Bullen A' Earth Model," *Bull. Seism. Soc. Amer.*, **58** (1968), 133-170.

2) Y. SATÔ and T. USAMI, "Propagation of Spheroidal Disturbances on an Elastic Sphere with a Homogeneous Mantle and a Core," *Bull. Earthq. Res. Inst.*, **42** (1964), 407-425.
T. USAMI and Y. SATÔ, "Theoretical Seismogram of Spheroidal Type on the Surface of a Homogeneous Gravitating Spherical Earth," *Bull. Earthq. Res. Inst.*, **44** (1966), 779-791.
Y. SATÔ, T. USAMI and M. LANDISMAN, "Theoretical Seismogram of Spheroidal Type on the Surface of a Gravitating Elastic Sphere. II. Case of Gutenberg-Bullen A' Earth Model," *Bull. Earthq. Res. Inst.*, **45** (1967), 601-624.

3) T. USAMI, Y. SATÔ, M. LANDISMAN and T. ODAKA, "Theoretical Seismograms of Spheroidal Type on the Surface of a Gravitating Elastic Sphere. III. Case of a Homogeneous Mantle with a Liquid Core," *Bull. Earthq. Res. Inst.*, **46** (1968), 791-819.

4) T. USAMI, Y. SATÔ and T. ODAKA, "Theoretical Seismogram and Earthquake Mechanism. I. Basic Principles. II. Effect of Time Function on Surface Waves," *Bull. Earthq. Res. Inst.*, **48** (1970), 533-579.

---

21. 重力均衡下にある弾性球の表面を伝わるスフェロイド型振動

IV. 緯度方向の力が流体核をもつ等質等方マントルに働いた場合

地震研究所 宇佐美龍夫
佐藤泰夫

1. 等質等方マントルと流体核からなる弾性球の表面に緯度方向の力が働いた場合に励起されるスフェロイド型振動の理論地震記象を計算し，前に計算した半径方向に力が働いた場合[1]と比較した．方法は前報と同じで多数の振動のモードを加え合せた．

2. 地球モデルとしては前報と同じものを使い，重力の影響を考慮した．また，擾乱の計算に使ったモードも同じで $i=1\sim10$ について周期 12 秒以上のものである．従つて，固有振動周期とそれから簡単な計算で求められる位相速度，群速度は前報と全く同じである．

3. 軸対称 $(m=0)$ を仮定し，外力としては極の附近で次のような緯度方向の力を表面に加えた．

$$F_{r\theta}=\Phi(\theta,\varphi)\cdot f(t)$$

$$\Phi(\theta,\varphi)=\Phi^0(\cos\theta)=\begin{cases}1 & \theta_1<\theta<\theta_2 \\ 0 & 0<\theta_1,\theta_2<\theta\end{cases}\quad\begin{pmatrix}\theta_1=0.006\\ \theta_2=0.012\end{pmatrix}$$

$$f(t)=\begin{cases}1/t_1 & |t|<t_1\\ 0 & t_1<|t|\end{cases}\qquad (t_1=0.004)$$

$$F_{\widehat{rr}}=0$$

時間の単位として（周長)/(表面における S 波速度)=6000 秒をとった．以上の条件の下でコモン・スペクトルを計算した．半径成分では基本モードに比して高調波のスペクトル振幅は遙かに小さい．余緯度成分では，周期の大きい（n が小さい）モードでは，高調波のスペクトルは基本モードのそれを凌駕する．また，その振幅は，半径方向の力が加わった前報に比して小さい．

4．これは，スフェロイド型振動は余緯度方向の力では起こしにくいことを意味する．n が大きいときに，この型の振動の励起振幅については近似的に（$\widehat{r\theta}$ なる力の場合）$\approx 1/n\times$（$\widehat{rr}$ なる力の場合）が成り立つ．但し，$\widehat{r\theta}$ と $\widehat{rr}$ は同じオーダーとする．

5．理論地震記象を地球上の数点で $t=0.001(0.001)1.000$，(即ち 6(6)6000 秒) について計算をした．前報に指摘した基本的な性質は，余緯度方向の力が加わったこの場合にも見出される．とくに注意すべき点は次の通り．

(a) 実体波では θ方向の振幅は r 方向の振幅より大きいが，半径方向の力が加わつた時には，この関係は逆になる．

(b) 表面波も実体波も振幅は半径方向の力が働いたときの 1/5～1/10 である．

(c) レイリー波の軌跡に，前報と同様，極での $\pi/2$ の位相のずれが見られる．